ECLÉTICA QUÍMICA

Eclet. Quim. 49 | e-1485, 2024

Original Article

https://doi.org/10.26850/1678-4618.eq.v49.2024.e1485

Influence of chitosan's purification methodology on the formation of layer-by-layer films

Ana Cristina Facundo de Brito **Pontes**[1+], Luciana Araújo **Nascimento**[1], Daniel de Lima **Pontes**[1], Ótom Anselmo de **Oliveira**[1], Francisco Ordelei da Silva **Nascimento**[1], Francimar Lopes da **Silva Júnior**[1]

Abstract

Concern for the environment for the development of new biodegradable materials has been constant in scientific circles. With this in mind, this work proposes a study on the formation of self-assembled thin films using chitosan (Qt), a biodegradable material. This polyelectrolyte has several purification methodologies, but we did not identify any studies on the effect of these methodologies on film formation. Thus, after the purification process and characterization of the three forms of chitosan purification, films were produced using the layer-by-layer (LBL) technique. The growth of the films was monitored using the UV-vis technique. Spectroscopy in the Infrared region showed positions in the main bands present in chitosan and sodium nitroprusside (NP) in the formed films. Two semi-reversible processes were found for the QtN/NP and QtAc/NP films, related to the reduction of iron oxide present in the NP. The effect of pH (4.0, 7.0 and 10) on the electrochemical processes indicated that the charge transfer occurs more efficiently at pH 7.0.

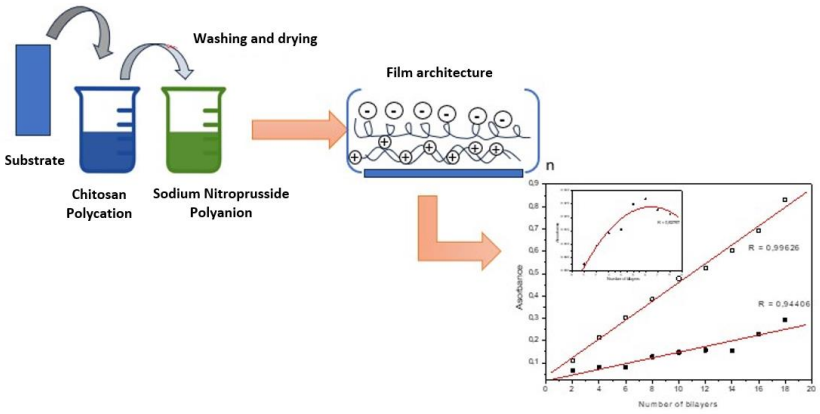

Article History

Received March 23, 2023
Accepted November 24, 2023
Published April 22, 2024

Keywords

1. biodegradable;
2. self-assembled;
3. sodium nitroprusside.

Section Editor

Patricia Hatsue Suegama
Marcos Carlos de Mattos

Highlights

- The effect of chitosan purification methodology.
- Monitoring the formation of self-assembled films by UV-Vis.
- Electrochemical tests indicate different interaction mechanisms between species.

[1]Federal University of Rio Grande do Norte, Institute of Chemistry, Natal, Brazil. **+Corresponding author:** Ana Cristina Facundo de Brito Pontes, **Phone:** +5584987166346, **Email address:** ana.cristina.pontes@ufrn.br

1. Introduction

The layer-by-layer (LBL) deposition represents an interesting alternative for the development of films for several applications such as medicine and bio-applications (Ariga *et al.*, 2012; Nesic *et al.*, 2016; Xia *et al.*, 2019) to improve corrosion resistance (Gao *et al.*, 2019) and electrochemical sensing and biosensing (Pannell *et al.*, 2018; Si *et al.*, 2019).

LBL method (Crespilho *et al.*, 2006a), has been the main choice for the manufacture of nanostructured films, as they have several advantages, such as low cost, various materials can be used, the film is made under mild conditions and thus, multilayer structures can be constructed to obtain the desired number of bilayers, since apparently there are no limitations on the amount of layers that can be deposited (Cheung *et al.*, 1992; Oliveira Junior *et al.*, 2001). The most common interaction is provided by the electrostatic attraction, the alternative adsorption of opposites charged. Due to their low toxicity, biodegradability, and natural availability (Umoren and Eduok, 2016) polysaccharides can be rather good candidates.

Chitosan in an acidic environment presents positive charges due to the protonation of the amino groups (NH_3^+), a substrate with a high density of negative sites immersed in this solution will behave as a suitable support for the attraction and subsequent formation of a homogeneous film. Layer-by-layer films with chitosan have been studied as active surfaces with antimicrobial and antioxidant potential (Li and Peng, 2015; Luo *et al.*, 2012).

Chitosan is the most well-known natural biopolymer and has a wide range of applications, such as in the health area (Delolo *et al.*, 2014; Lins *et al.*, 2014; Silva *et al.*, 2006; Ungureanu *et al.*, 2015), environment (Marques Neto *et al.*, 2013) and technology (Souza *et al.*, 2015; Vinhola *et al.*, 2012).

The properties of chitosan, such as degree of purity, solubility, viscosity, degree of deacetylation (GD), molecular weight and others, are influenced by the methodology used to obtain it, as well as by the purification techniques to which they are subjected (Arrascue *et al.*, 2003; Battisti and Campana-Filho, 2008; Crini and Badot, 2008; Santos *et al.*, 2003; Gonsalves *et al.*, 2011; Kumar, 2000; Laranjeira and Fávere, 2009; Roberts, 1992; Silva *et al.*, 2006).

There are several methodologies used for the purification of chitosan, however, these procedures involve the steps of dissolving in an aqueous medium of controlled ionic strength, filtration, precipitation by the addition of non-solvent, washing and drying. This type of purification defines in advance the type of counter ion that will be present in the purified sample. Steps such as dialysis and lyophilization can be added to the procedures (Signini and Campana Filho, 2001).

As in the layer-by-layer technique, the production of films is based on the electrostatic interaction between molecules containing ionic groups and having chitosan as the amino group (NH_3^+), it is necessary to use another compound with opposite charge. Thinking about the production of films that may have applications as biosensors, NP was used, with molecular formula $Na_2[Fe(CN)_5(NO)]$. It has been used for more than 50 years as a vasodilator in cases of emergency in hypertension attacks, blood pressure control in surgeries and the treatment of chronic hypertension as it provides a quick response without the need for overuse (César *et al.*, 2001; Freitas *et al.*, 2012; Sass *et al.*, 2007; Stocche *et al.*, 2003). There are also reports of the use of NP in the determination of sulfur compounds in fresh and saline waters (Sonne and Dasgupta, 1991), as well as in the determination of phenols in aqueous two-phase systems (Rodrigues *et al.*, 2010).

The literature reports several types of film formation studies with chitosan, however, they all use it with modifications, whether in the form of Schiff bases or through crosslinking reactions (Amanulla *et al.*, 2017; Lu *et al.*, 2022; Suginta *et al.*, 2013). Therefore, this article makes a study on the effect of chitosan purification on the formation of self-assembled films obtained through electrostatic interaction.

2. Experimental

2.1. Chitosan purification

Chitosan of commercial origin (POLYMAR) was purified in three different ways, to obtain a pure and homogeneous material. The methodologies used in the purifications were proposed by Signini and Campana Filho (2001) with modifications and are described below:

a. **Neutral chitosan ($Qt_{Neutral}$):** It is solubilized in acetic acid, precipitated in ammonium hydroxide, filtration, dried, and stored in a dry environment.
b. **Chitosan acetate ($Qt_{Acetate}$):** It is solubilized in acetic acid, precipitated in ethanol, dried, and stored in a dry environment.
c. **Chitosan hydrochloride ($Qt_{Hydrochloride}$):** Solubilized in hydrochloric acid, sodium chloride added, precipitated in ethanol, filtered, dried, and stored in a dry environment.

2.2. Chitosan characterization

The infrared spectra of chitosan purified in different forms were obtained in the form of a KBr tablet, using a Shimadzu spectrophotometer, model FTIR-8400S, series IRAFFINITY-1, software IRSOLUTION, version 1.60, with scan number equal to 30 and resolution 4.

The determination of the degree of deacetylation of the purified chitosan (% GD) was made by conductivity measurement (Raymond *et al.*, 1993), and the viscometrical molar mass was obtained through capillary viscosimetry (Signini and Campana Filho, 1998; 2001). The values of the Huggins constant (K) and α used were 76.0×10^{-5} and 0.76 (Canella and Garcia, 2001).

The moisture percentage of chitosan samples was determined by thermogravimetric analysis using a thermogravimetric analyzer unit and simultaneously calorimeter, TA Instruments model SDTQ600 manufacturer. The samples were analyzed in an alumina crucible at a rate of 2.5 °C min^{-1}, heated from 25 °C to 900 °C under a nitrogen atmosphere, with a flow rate of 50 mL min^{-1}.

2.3. Sodium nitroprusside (NP)

The $Na_2[Fe(CN)_5(NO)]$ used was obtained from PROQUÍMIOS and no purification was necessary. For the preparation of the films, a solution of 23 g L^{-1} in methanol was prepared.

2.4. Layer-by-layer (LBL) fabrication

The LBL films were deposited on quartz and ITO glass substrates by alternating immersion into cationic chitosan and anionic NP solutions for 5 min. Chitosan solution (Qt) 5 g L^{-1} in 1% acetic acid and a solution of sodium

nitroprusside (NP) 23 g L^{-1} in methanol. After each dive, the slide was washed with distilled water and dried under nitrogen flow. The films were prepared with $(Qt/NP)_n$, with "n" being the number of layers with n = 2, 4, 18 and 20 layers.

2.5. Characterization of LBL films

The growth monitoring of the films was performed using the UV-Vis absorbance spectroscopy technique (Agilent, model 8453) on a quartz plate, the same material used in the IR technique for LBL films using the Shimadzu spectrophotometer, model FTIR-8400S, series IRAFFINITY-1, software IRSOLUTION, version 1.60, with scan number equal to 30 and resolution 4.

The electrochemical experiments were performed using an AUTOLAB AUT 85282 system. The film $(Qt/NP)_{20}$ was deposited on ITO (glass covered with a thin indium-doped tin oxide layer) glass substrates used as a working electrode. The reference electrode was an Ag|AgCl/KCl saturated electrode and the counter electrode was a Pt plate The electrochemical cell used in the cyclic voltammetry measurements had a total volume of 50 mL with a cap with a plug for 3 electrodes and before the measurement, argon gas was bubbled into the solution. The experiments were conducted in a 0.1 mol L^{-1} KCl at 25 °C.

3. Results and discussion

The purification process of chitosan in neutral, acetate and hydrochloride forms yielded 82.5%, 64.1% and 85.6%, respectively. These yield values are due to loss due to handling and, mainly, to the presence of insoluble materials and aggregates present in chitosan that were eliminated during the filtration steps. The presence of insoluble materials in commercial products is reported in the literature (Ottøy *et al.*, 1996).

The purification process makes more polar groups available, which increases the ability to interact with other compounds (Signini and Campana Filho, 2001). The differences in purification methodologies resulted in different chitosan molecules in terms of visual aspect and solubility. All the purified samples were soluble in diluted acetic acid solution, the samples purified in the form of acetate and hydrochloride were partially soluble in water.

The number of amino groups present in the chitosan polymer chain is an important parameter and is related to electrostatic interactions for the formation of self-assembled films. Its order of magnitude can be determined through the degree of deacetylation (% GD). One of the simplest and most used techniques for this determination is conductometric titration. The data obtained for the different chitosan samples are shown in **Table 1**. The lower % GD of the $Qt_{Hydrochloride}$ sample can be explained by the change in inter- and intra-chain relationships, caused by using a strong acid in its purification.

The moisture content for the purified chitosan samples in the different forms obtained values lower than that observed in the literature (Signini and Campana Filho, 2001) (23.8 ±0.4) % for the same purification methodology. The difference may be related to the drying step, in the case of literature it was carried out at 25 °C, which does not remove the water present, whereas, in our work, the drying process was used with slight heating.

Viscosimetry is one of the most used processes for determining the molar mass of polymers, as it is a simple technique without requiring equipment with high costs. For the three purified chitosan holders, a good correlation index was obtained between the experimental measures with R > 0.99. As can be seen in **Table 1**, the application used in the purification of chitosan directly affects the viscosity of the polysaccharide and its molar mass, indicating differences in its properties.

Table 1. Chitosan properties in its different forms of purification.

Sample	% GD	η (mL g^{-1})	Mv(g mol^{-1})	Mv (g mol^{-1})*	Moisture content (%)
$Qt_{Neutral}$	68 ± 2	273.72	4.79 x 10^4	16.7 x 10^4	12.16
$Qt_{Neutral}$	69 ± 5	136.18	1.14 x 10^4	17.2 x 10^4	13.49
$Qt_{Hydrochloride}$	61 ± 4	44.72	4.54 x 10^3	16.1 x 10^4	16.84

Source: Elaborated by the authors using data from Signini and Campana Filho (2001).

The main characteristic bands of the infrared absorption spectrum of samples of chitosan in their different purified forms are shown in **Table 2**. The OH axial stretch band, between 3467 to 3502 cm^{-1}, appears to overlap the band N-H stretch. All bands identified are very similar to those described in the literature (Battisti and Campana-Filho, 2008; Vinhola *et al.*, 2012) and show that the same functional groups are present in all analyzed samples. The band in the 2926 to 2030 cm^{-1} region is attributed to the C-H stretching of the CH_2 groups of pyranoses. It is also possible to observe a peak from 1321 cm^{-1} to 1381 cm^{-1} characteristic of the angular deformation of CH_2 and CH_3.

Table 2. Main assignments of the infrared bands for the purified chitosan samples.

Sample	Infrared band assignments (cm^{-1})							
	$\nu_{C=O}$ (amide I)	δ_{N-H} (amide II)	δ_{C-N} (amide III)	δ_{CH}	ν_{COC} β-(1-4)	δ_{CO}	ν_{OH}	ν_{C-H}
$Qt_{Neutral}$	1664	1556	1381	1423	1156	1078	3467	2878
$Qt_{Acetate}$	1658	1566	1321	1415	1157	1074	3471	2879
$Qt_{hydrochloride}$	1643	1525	1381	1323	1155	1082	3502	2885
Signini and Campana Filho (2001)	1655	1600	1423	-	1153	1031	3450	2904

Note: δ = deformation; ν = Stretch.
Source: Elaborated by the authors using data from Signini and Campana Filho (2001).

The thermal analysis study for the chitosan samples in their different forms of purification showed two mass losses. The first event is related to the loss of moisture in the material, while the second event is related to the breaking of the polymer bonds, these occurred at 273.8, 260.3 °C and 185.6 °C for Qt_{neural}, $Qt_{Acetate}$ and $Qt_{hydrochloride}$, respectively.

3.2. Characterization of Sodium Nitroprusside (NP)

The infrared spectrum for sodium nitroprusside showed bands at 2161, 2158 e 2144 cm^{-1} related to the stretching vibrations of the cyanide ligand, another characteristic band of this complex is the NO stretch identified at 1942 cm^{-1}. In the region of the infrared spectrum below 700 cm^{-1}, it is possible to identify the signals attributed to the metal, so in 495 and 423 cm^{-1} bands related to the Fe-C≡N bond and Fe-C in 466 cm^{-1}. The very intense band at 661cm^{-1} is attributed to linear deformation Fe-N→O, all these bands follow what has been reported in the literature for complex (Palliani *et al.*, 1971).

The electronic spectrum of NP at 23 g L^{-1} (0.106 mol L^{-1}) in methanol is shown in **Fig. 1**, where initially only two bands are observed, the first at 208 nm related to the $d_{xy}\rightarrow\pi^*CN$ transition and the second at 270 nm attributed to d_{xz}, $d_{yz} \rightarrow d_z^2$. It was necessary to prepare higher concentrations to identify the band related to the $d_{xy}\rightarrow\pi^*NO$, transition, identified at 540 nm as can be seen in **Fig. 1a**. The 270 nm band was used to monitor the growth of the films since it is possible to monitor them at low concentrations (Palliani *et al.*, 1971; Swinehart, 1967).

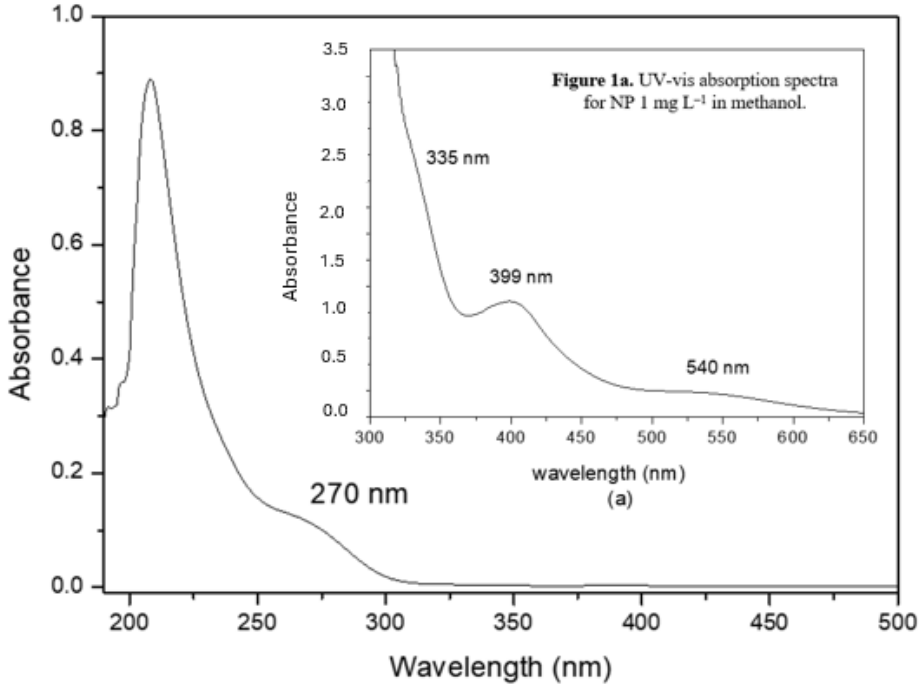

Figure 1. UV-vis absorption spectra for NP 0.03 mg L^{-1} and **(1a)** for NP 0.2 mg L^{-1} in methanol.

3.3. Characterization of LBL films

The deposition of materials in the LBL film formation process was investigated by monitoring its increase in absorbance after the preparation of each bilayer. This procedure makes it possible to assess whether the materials are deposited in quantities like each formed bilayer.

For all Qt/NP films, prepared with the three purification methodologies, have UV-vis absorption around 270 nm, this band is related to the electronic transition of NP (d_{xz}, $d_{yz} \rightarrow d_z^2$). The deposition of materials in the process of forming self-assembled films was investigated using its absorbance technique after the preparation of each bilayer, as shown in **Fig. 2** for $Qt_{Neutral}$/NP.

The thickness of the films can be controlled by the number of bilayers deposited and the polymer used. If linear growth is observed, it indicates that the same amount of material is adsorbed in each deposition step (Eiras *et al.*, 2007). **Figure 3** shows the relationship between absorbance and the number of layers formed for the three Qt purification methodologies. There is a linear growth for the three formed films, however with different slopes. The films obtained with Qt in neutral form and acetate obtained better correlation and slope indexes, according to Eiras *et al.* (2007), greater slopes in these graphs are related to greater affinities between the compounds that form a layer. Thus, we can conclude that among the three methodologies used in the purification, $Qt_{Acetate}$ showed a greater affinity with NP for the formation of self-assembled films and $Qt_{Hydrochloride}$ is the one with less affinity.

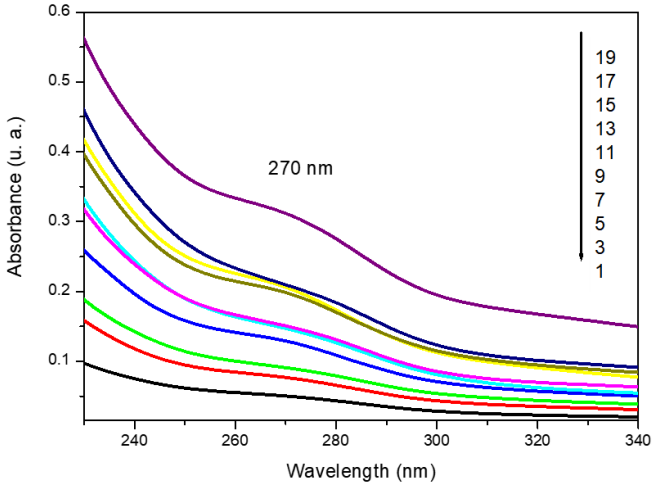

Figure 2. The electronic absorption spectrum in the UV-vis region of the films self-assembled with an increasing number of layers ($Qt_{Neutral}$/NP) prepared from a solution of Qt 5 g L^{-1} and NP 23 g L^{-1}.

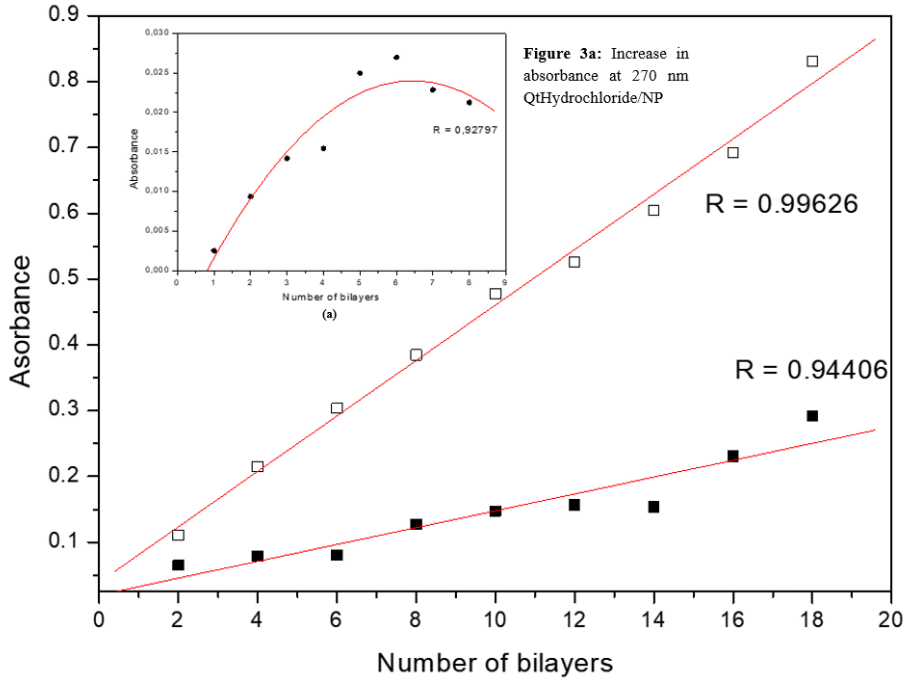

Figure 3. Increase in absorbance at 270 nm as a function of the number of bilayers of self-assembled films to $Qt_{Neutral}$/NP (■), $Qt_{Acetate}$/NP (□) and **(3a)** QtHydrochloride/NP (●) prepared from a solution of Qt 5 g L^{-1} and NP 23 g L^{-1}.

The more similar the amounts adsorbed in each adsorption step, the higher the value of the correlation index (R) (**Table 3**) because the closer the points are to the line. Thus, it can be observed that the film formed from $Qt_{Acetate}$ has a linear behavior of deposition of materials on the solid substrate with the number of layers, that is, the same amount of material is deposited in each step (Eiras *et al.*, 2007), for films containing $Qt_{Neutral}$ it presented an exponential behavior. Picart *et al.* (2002) demonstrated that growth can occur linearly or exponentially due to the ability of at least one of the polyelectrolytes to diffuse in and out of the film. This author monitored the growth of films using Poly-L-lysine and identified that it was present in the outermost layer of the film. Regarding the film obtained with $Qt_{Hydrochloride}$, an irregular behavior of deposition of the material in the film is noticed.

The observed data clearly indicate that the methodology used in the purification of chitosan directly influences the formation of films with the complex. According to Signini and Campana Filho (2001), the chitosan purified in the form of hydrochloride has charges that will alter the inter and intricate interactions, modifying its arrangement, these changes seem to disadvantage the formation of the chitosan film, as it presents a random growth probably caused by the inadequate electrostatic interactions between chitosan and the complex.

Table 3. Slope data and correlation indexes of the films of neutral chitosan, acetate, and hydrochloride with NP.

Purified form of Qt	Inclination	Correlation Index
$Qt_{Neutral}$	0.01280	0944.06
$Qt_{Acetate}$	0.04034	0.99737
$Qt_{Hydrochloride}$	0.00293	0.85615

The Spectroscopy technique in the Infrared region was also used to evidence the species present in the films, **Table 4** shows the main attributions for the Qt/NP film with 20 bilayers. In general, the spectra showed displacements, probably caused by the interaction between Qt and NP.

The N-H (1566 cm^{-1}) stretch characteristic of chitosan suffered displacements in the films of $Qt_{Neutral}$ (1556 cm^{-1}) and $Qt_{Acetate}$ (1556 cm^{-1}), respectively. The stretch attributed to NO present in the film was displaced to 1931 cm^{-1}, the Fe-C≡N deformation also showed a small displacement (**Table 4**). The characteristic band of the C-H stretching undergoes small shifts compared to the spectrum of purified chitosan, which was expected as it is an indication of a modification in its neighborhood.

The results of spectroscopy and UV-vis suggest that both chitosan and NP are being deposited in layers for the formation of the films and that this interleaving is directly related to the type of purification that the chitosan has undergone.

Table 4. Band assignments observed in the IR spectrum for chitosan films with NP.

Assignment	Film $Qt_{Neutral}$/NP	Film $Qt_{Acetate}$/NP	Film $Qt_{Hydrochloride}$/NP
ν_{OH}	3394	3398	3480
ν_{C-H}	2924	2928	2840
$\nu_{-C\equiv N}$	2141	2140	2152
$\nu_{COC\ \beta\text{-}(1\text{-}4)}$ or δ_{CO}	1122	1070	1156
δFe-C≡N	482	482	500
ν_{NO}^{+}	1931	1931	1940
δFe-N→O	471	488	490

The study on the thermal stability of chitosan in different forms of purification and Qt/NP films was carried out, except for the $Qt_{Hydrochloride}$/NP film, considering that the results obtained by UV-vis spectroscopy, since it did not show good interaction between chitosan and NP.

Figure 4 shows thermogravimetry (TG) and derivative thermogravimetry (DTG)for films Qt/NP, the moisture content in the films was 13.94% for $Qt_{Neutral}$ and 16.92% for $Qt_{Acetate}$. A second event is observed in the films at 174 and 182 °C for $Qt_{Neutral}$ and $Qt_{Acetate}$, respectively. Osiri *et al.* (2015) report that there is a loss of mass in coordination compounds containing cyanide and nitrosyl

as a binder at temperatures close to 190 °C, thus we can infer that the mass losses previously mentioned are related to the decomposition of NP present in the films, coupled with the fact of these losses of mass are not seen in the purified chitosan.

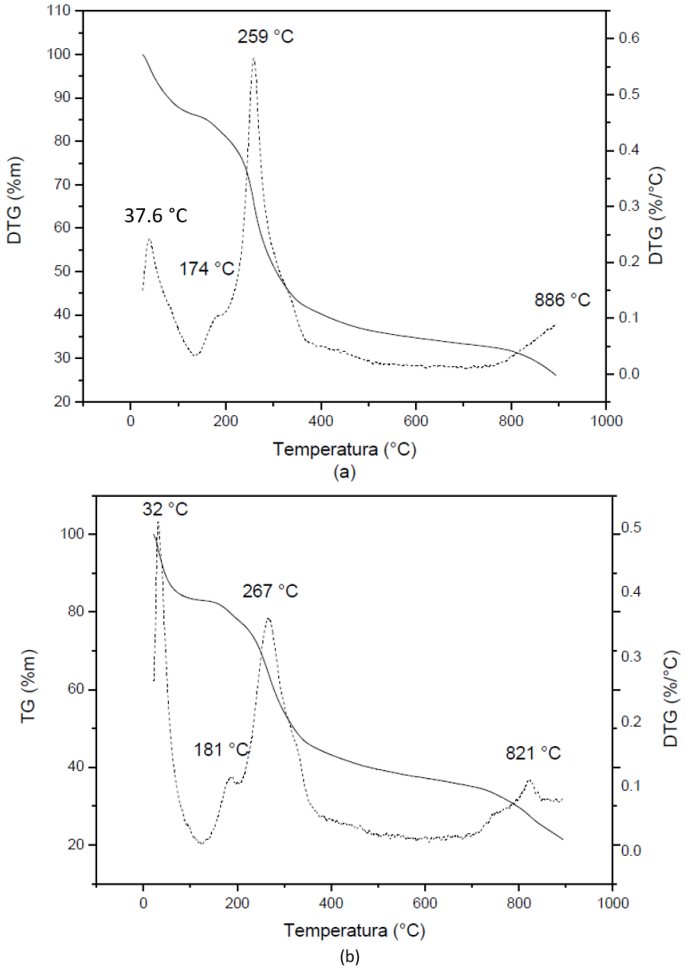

Figure 4. TG (solid) and DTG (dot) curves of **(a)** $Qt_{Neutral}$/NP e **(b)** $Qt_{Acetate}$/NP analyzed in an alumina crucible at a rate of 2.5 °C min^{-1}, heated from 25 to 900 °C under a nitrogen atmosphere, with a flow rate of 50 mL min^{-1}.

A third event is observed at temperatures above 250 °C which is related to the breakdown of glycosidic bonds, followed by the decomposition of the acetylated and deacetylated units (Martínez-Camacho *et al.*, 2010; Martins *et al.*, 2012; Nesic *et al.*, 2016). It was observed that in general the addition of the complex for the formation of self-assembled films decreased the thermal stability of chitosan. It is also possible to identify an event occurring at a temperature of 866 and 820 °C for $Qt_{Neutral}$ and $Qt_{Acetate}$, respectively, this event is related to NP degradation. A comparison of the decomposition temperatures for the different samples is shown in **Table 5**.

Table 5. Results of thermogravimetric analysis.

	1st mass loss (°C)	2nd mass loss (°C)	3rd mass loss (°C)	4th mass loss (°C)
$Qt_{Neutral}$	35.0	-	273.8	-
$Qt_{Neutral}$/NP	37.6	174	259.0	886.0
$Qt_{Acetate}$	35.4	-	260.3	-
$Qt_{Acetate}$/NP	32.0	181	267.0	821.0

Thus, it is possible to identify that the methodology used in the purification of chitosan plays an important role in the formation of LBL films with NP.

3.4. Cyclic voltammetry of LBL films

The cyclic voltammetry study in LBL films (20 layers) of chitosan purified in the form of acetate and neutral with the complete ones deposited on the ITO surface was analyzed in saline medium (KCl 0.1 mol L^{-1}). To evaluate the influence of the chitosan form of purification on the electrochemical response, a study was made of the current variation as a function of the applied potential. The $Qt_{Hydrochloride}$ sample was not characterized by the cyclic voltammetry technique, since it did not present good results in the deposition for forming the films.

The analysis of voltammograms showed that as the scanning speed increases, there is an increase in the value of the anodic and cathodic peak currents. It was observed that at 50 mV s^{-1} the electrochemical spectrum had higher resolution and the potentials could be determined with greater accuracy, that is, it presented a fast response, without loss of precision in detecting the anodic peak potentials (E_{pa}) and cathodic (E_{pc}), as well as anodic (i_{pa}) and cathodic (i_{pc}) peak currents. **Figure 5** shows the voltammetric profiles for the films of $Qt_{Neutral}$/NP and $Qt_{Acetate}$/NP, presenting 2 peaks, one of oxidation and one of reduction related to the redox process (Fe(III)/Fe(II) of the metal present in the complex. For the $Qt_{Neutral}$/NP film the anodic and cathodic peak values were 0.59 and 0.44 V, respectively, whereas for $Qt_{Acetate}$/NP we obtained the values of 0.62 and 0.45 V. Generally, small displacements are observed, for the film formed with the neutral chitosan, a displacement of 0.04 V was observed for the anodic peak when compared to the values obtained for the NP film (oxidation at 0.63 V and reduction at 0.50 V). It is possible to observe a small shift in the anodic peak towards more positive potentials and a shift in the cathodic peak towards more negative potentials; this behavior is characteristic of quasi-reversible processes. Another important aspect is the stability of these electrodes after carrying out several measurements. After electrochemical measurements, the electrolyte solution was analyzed using the UV-vis technique and no band was observed, confirming that there is no migration of the components to the electrolyte and indicating that the films are stable.

https://doi.org/10.26850/1678-4618.eq.v49.2024.e1485

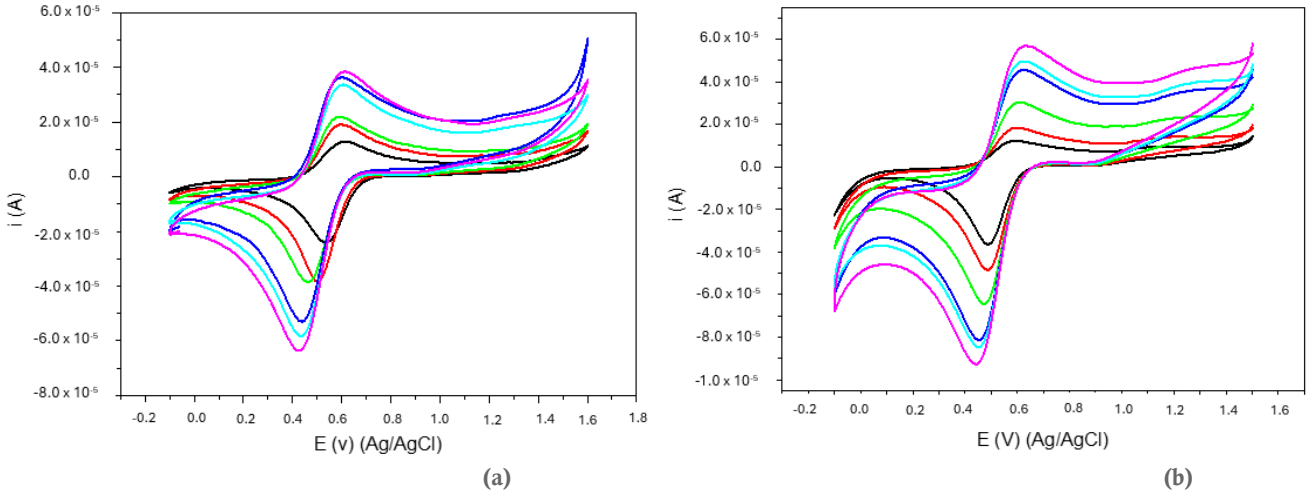

Figure 5. Cyclic voltammograms for 20-bilayer **(a)** $Qt_{Neutral/NP}$ and **(b)** $Qt_{Acetate/NP}$ on ITO with multiple scans rates: (—) 5 mV s^{-1}; (—) 10 mV s^{-1}; (—) 25 mV s^{-1}; (—) 50 mV s^{-1}; (—) 75 mV s^{-1}; (—) 100 mV s^{-1}. Electrolyte: KCl 0.1 mol L^{-1}.

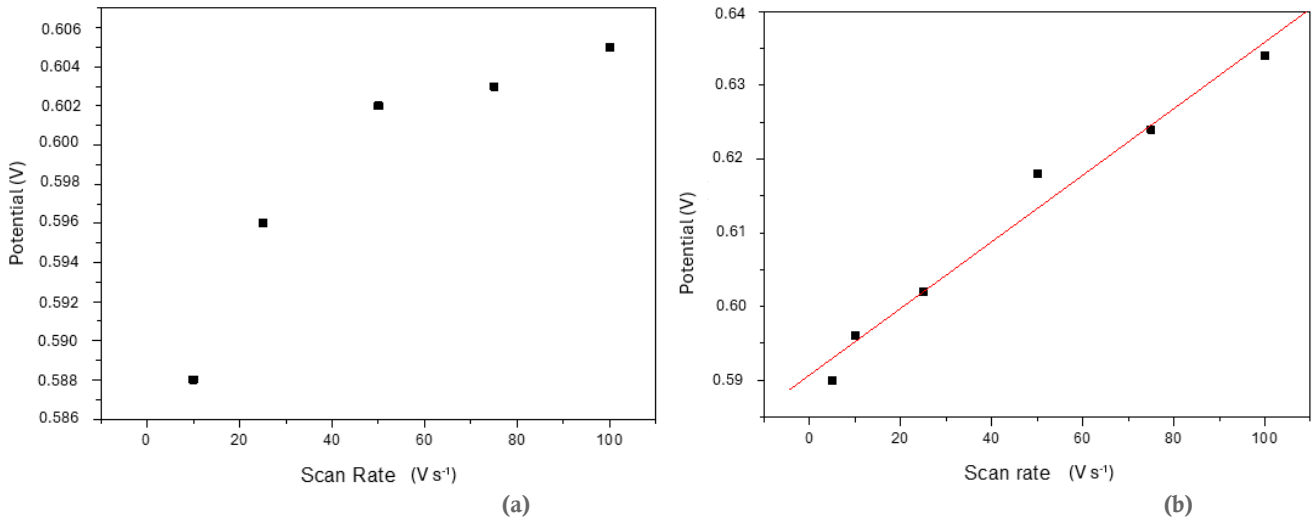

Figure 6. Monitoring the oxidation peak potential with the scan rate for 20-bilayer **(a)** $Qt_{Neutral}$/NP and **(b)** $Qt_{Acetate}$/NP on ITO in KCl 0.1 mol L^{-1} at 50 mV s^{-1}.

The anodic peak potential increases linearly with the scan rate for the $Qt_{Acetate}$/NP film, as can be seen in **Fig. 6b**, with a correlation index of 0.98807 and for $Qt_{Neutral}$/NP (**Fig. 6a**) different behavior is observed. Study of chitosan/FeTsPc and chitosan/NiTsPc films (Crespilho *et al.*, 2006b) an increase in anodic potential was observed with the scan rate, even according to the author, this behavior is evidence of a load transport mechanism, like the results obtained for the $Qt_{Acetate}$/NP film. For the films formed by $Qt_{Neutral}$/NP, the diffusion process occurs, since there is no linear behavior with the scan rate.

Also, according to Crespilho *et al.* (2006b), for LBL films formed by chitosan/FeTsPc and chitosan/NiTsPc molecules, the type of mechanism that occurs is electron hopping, since the interaction between species is the ionic interaction between the groups amino of chitosan and the phthalocyanic sulfonic groups present in the complexes. This same type of interaction is proposed for films containing $Qt_{Acetate}$/NP, between the chitosan amino group and the $[Fe(CN)_5NO]^{-2}$ of the complex.

The value of ΔEp as a function of the scan rate is shown in **Fig. 7**, in which it is possible to observe that only the $Qt_{Neutral}$/NP film can be considered as a semi-reversible process since the potential values increased with the increase of scan rate. The graphic (**Fig. 7**) makes clear that the methodology used in the purification of chitosan directly influences the interaction and formation of thin films.

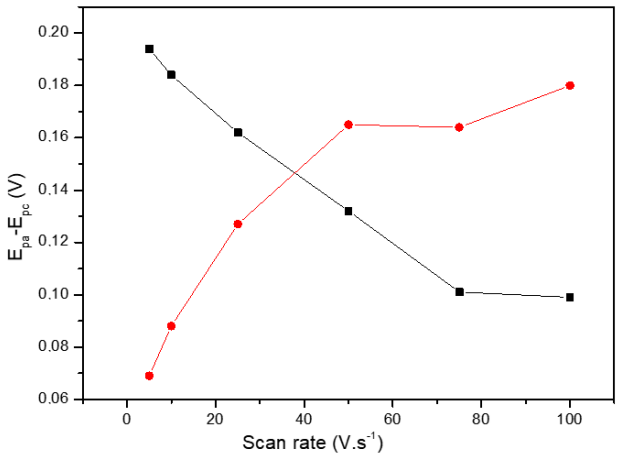

Figure 7. Relationship of potential variation (ΔEp) versus scan rate for $Qt_{Neutral}$/NP (■) e $Qt_{Acetate}$/NP (●).

The study of the effect of pH (4.0; 7.0 and 10) on the electrochemical behavior of the $Qt_{Neutral}$/NP and $Qt_{Acetate}$/NP films was carried out and the results are shown in **Fig. 8**. It is possible to observe that at pH 4, the obtained films did not present a good electrochemical response, making it difficult to identify the anodic process. At pH 10 divergence is observed in the electrochemical behavior for the films purified in different ways, for the $Qt_{Neutral}$/NP film it is not possible to identify the anodic process, different behavior for the $Qt_{Acetate}$/NP film, in which a displacement of the cathodic peaks is observed and anodic for 0.73 V and 0.19 V, respectively. These results indicate that the charge transfer process occurs more efficiently at pH equal to 7.0 for the different forms of purification.

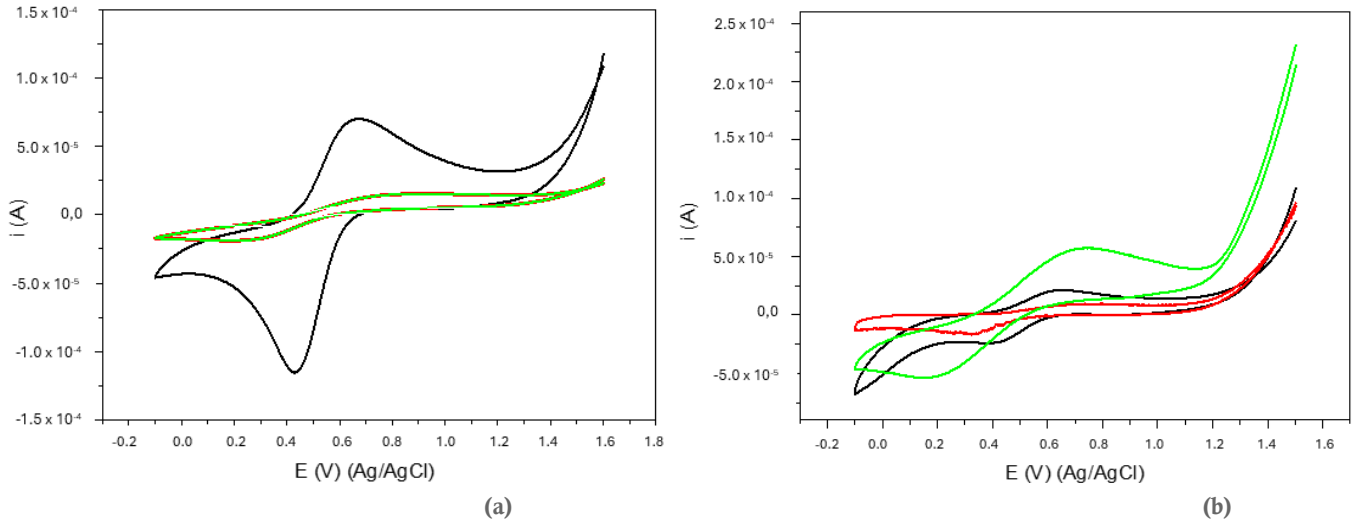

Figure 8. Cyclic voltammograms obtained for **(a)** $Qt_{Neutral}$/NP **(b)** $Qt_{Acetate}$/NP in pH (—) 4.0; (—) 7.0 e (—) 10 with scan rate de 50 mV s^{-1}.

To identify if there was any change in the self-assembled films' thermal stability after the electrochemical study, thermal analysis tests were performed. It was possible to observe that the thermal stability (**Table 6**) of the films did not undergo any significant change, which may indicate the films are stable after being polarized i.e., after using in the form of electrodes.

Table 6. Data thermal analysis after voltammetry.

	1st mass loss (°C)	2nd mass loss (°C)	3rd mass loss (°C)	4rd mass loss (°C)
$Qt_{Neutral}$/NP	40.0	179	257.8	887.9
$Qt_{Acetate}$/NP	31.7	183.1	263.1	820.0

4. Conclusions

The methodology used in the purification of chitosan produced materials with different characteristics such as molar mass, viscosity, humidity, and degree of deacetylation. These characteristics seem to directly interfere with the deposition of layers for the formation of LBL films, as evidenced by UV-vis techniques, in which the chitosan purification methodology in the form of hydrochloride was the one that showed deposition of the material in the film completely random and, therefore, it was not used for the characterization of the electrochemical profile. The $Qt_{tneutra}$/NP film, presented an exponential growth, indicating that one of the polyelectrolytes can diffuse between the layers of the film, as far as the growth of the $Qt_{Acetate}$/NP film was linear. Differences regarding the thermal stability of the films were also identified, in which the film formed by $Qt_{tneutra}$/NP was the one that presented a greater reduction in the decomposition temperature, of approximately 15 °C when compared to purified chitosan. Through this technique it was also possible to identify the loss of mass related to the NP, confirming once again its presence in the film, as also observed by the spectroscopy technique in the infrared region.

The electrochemistry tests showed that the $Qt_{Neutral}$/NP and $Qt_{Acetate}$/NP films when used as working electrodes are stable and that there is no migration of their components to the electrolyte. Studies of thermal analysis of the films after electrochemical tests showed changes in relation to its decomposition temperatures. There was a shift towards more positive potentials of the anodic peak when compared to NP under the same conditions for $Qt_{Neutral}$/NP, whereas with respect to the cathodic peak the difference of 0.05 V was the same observed for the two films. There are distinct interactions and behaviors between the two films corroborating the UV-vis results. The $Qt_{Neutral}$/NP film presents a semi-reversible process while the other is reversible, indicating differences in the charge transfer process between the two films. For the $Qt_{Acetate}$/NP film the charge transport occurs, while for the $Qt_{Neutral}$/NP film the diffusion process occurs. In addition, pH equal to 7 proved to be ideal for electrochemical measurements.

Authors' contributions

Conceptualization: Pontes, A. C. F. B.; **Data curation:** Nascimento, L. A.; Silva Júnior, F. L.; **Formal Analysis:** Nascimento, L. A.; Silva Júnior, F. L.; Pontes, A. C. F. B.; **Funding acquisition:** Pontes, A. C. F. B.; Pontes, D. L.; Oliveira, O. A.; Nascimento, F. O. S.; **Investigation:** Nascimento, L. A.; Silva Júnior, F. L.; Pontes, A. C. F. B.; **Methodology:** Nascimento, L. A.; Pontes, A. C. F. B.; **Project administration:** Nascimento, L. A.; Silva Júnior, F. L.; Pontes, A. C. F. B.; Pontes, D. L.; Oliveira, O. A.; **Resources:** Pontes, A. C. F. B.; Pontes, D. L.; Oliveira, O. A.; Nascimento, F. O. S.; **Software:** Not applicable; **Supervision:** Pontes, A. C. F. B.; **Validation:** Not applicable; **Visualization:** Pontes, A. C. F. B.; **Writing – original draft:** Pontes, A. C. F. B.; Silva Júnior, F. L.; Pontes, D. L.; Oliveira, O. A.; Nascimento, F. O. S.; **Writing – review & editing:** Pontes, A. C. F. B.

Data availability statement

All data sets were generated or analyzed in the current study.

Funding

Not applicable.

Acknowledgments

The Analytical Center of the Chemistry Institute of UFRN for the use of the equipment used in this work.

References

Amanulla, B.; Palanisamy, S.; Chen, S.-M.; Chiu, T.-W.; Velusamy, V.; Hall, J. M.; Chen, T.-W.; Ramaraj, S. K. Selective Colorimetric Detection of Nitrite in Water using Chitosan Stabilized Gold Nanoparticles Decorated Reduced Graphene oxide. *Sci. Rep.* **2017**, *7* (9) 1–9. https://doi.org/10.1038/s41598-017-14584-6

Ariga, K.; Ji, Q.; McShane, M. J.; Lvov, Y. M.; Vinu, A.; Hill, J. P. Inorganic nanoarchitectonics for biological applications. *Chem. Mater.* **2012**, *24* (5), 728–737. https://doi.org/10.1021/cm202281m

Arrascue, M. L.; Garcia, H. M.; Horna, O.; Guibal, E. Gold sorption on chitosan derivatives. *Hydrometallurgy*. **2003**, *71* (1–2), 191–200. https://doi.org/10.1016/S0304-386X(03)00156-7

Battisti, M. V.; Campana-Filho, S. P. Obtenção e caracterização de α-quitina e quitosanas de cascas de Macrobrachium rosembergii. *Quim. Nova.* **2008**, *31* (8), 2014–2019. https://doi.org/10.1590/S0100-40422008000800019

Canella, K. M. N. D. C.; Garcia, R. B. Caracterização de quitosana por cromatografia de permeação em gel -Influência do metodo de preparacao e do solvente. *Quim. Nova.* **2001**, *24* (1), 13–17. https://doi.org/10.1590/S0100-40422001000100004

César, D. S.; Miyoshi, E.; Halpern, H.; Auler, J. Fenoldopam: Novo antihipertensivo parenteral; alternativa ao nitroprussiato. *Rev. Bras. Anestesiol*. **2001**, *51* (6), 528–536. https://doi.org/10.1590/s0034-70942001000600008

Cheung, J. H.; Punkka, E.; Rikukawa, M.; Rosner, R. B.; Royappa, A. T.; Rubner, M. F. New developments in the Langmuir-Blodgett manipulation of electroactive polymers. *Thin Solid Films.* **1992**, *210–211* (Part 1), 246–249. https://doi.org/10.1016/0040-6090(92)90224-Y

Crespilho, F. N.; Zucolotto, V.; Siqueira, J. R.; Carvalho, A. J. F.; Nart, F. C.; Oliveira Junior, O. N. Using electrochemical data to obtain energy diagrams for layer-by-layer films from metallic phthalocyanines. *Int. J. Electrochem. Sci.* **2006a**, *1* (4), 151–159. https://doi.org/10.1016/S1452-3981(23)17145-8

Crespilho, F. N.; Zucolotto, V.; Oliveira Junior, O. N.; Nart, F. C. Electrochemistry of layer-by-layer films: A review. *Int. J. Electrochem. Sci.* **2006b**, *1* (5), 194–214. https://doi.org/10.1016/S1452-3981(23)17150-1

Crini, G.; Badot, P. M. Application of chitosan, a natural aminopolysaccharide, for dye removal from aqueous solutions by adsorption processes using batch studies: A review of recent literature. *Prog. Polym. Sci.* **2008**, *33* (4), 399–447. https://doi.org/10.1016/j.progpolymsci.2007.11.001

Delolo, F. G.; Rodrigues, C.; Silva, M. M.; Dinelli, L. R.; Delling, F. N.; Zukerman-Schpector, J.; Batista, A. A. A new electrochemical sensor containing a film of chitosan-supported ruthenium: Detection and quantification of sildenafil citrate and acetaminophen. *J. Braz. Chem. Soc.* **2014**, *25* (3), 550–559. https://doi.org/10.5935/0103-5053.20140031

Eiras, C.; Passos, I. N. G.; Brito, A. C. F.; Santos Júnior, J. R.; Zucolotto, V.; Oliveira Junior, O. N.; Kitagawa, I. L.; Constantino, C. J. L.; Cunha, H. N. Nanocompósitos eletroativos de poli-o-metoxianilina e polissacarídeos naturais. *Quim. Nova.* **2007**, *30* (5), 1158–1162. https://doi.org/10.1590/S0100-40422007000500020

Freitas, A. F.; Bacal, F.; Oliveira, J. L.; Fiorelli, A. I.; Santos, R. H.; Moreira, L. F. P.; Silva, C. P.; Mangini, S.; Tsutsui, J. M.; Bocchi, E. A. Sildenafil vs. Sodium before nitroprusside for the pulmonary hypertension reversibility test before cardiac transplantation. *Arq. Bras. Cardiol.* **2012**, *99* (3), 848–856. https://doi.org/10.1590/S0066-782X2012005000076

Gao, F.; Hu, Y.; Gong, Z.; Liu, T.; Gong, T.; Liu, S.; Zhang, C.; Quan, L.; Kaveendran, B.; Pan, C. Fabrication of chitosan/heparinized graphene oxide multilayer coating to improve corrosion resistance and biocompatibility of magnesium alloys. *Mater. Sci. Eng. C.* **2019**, *104*, 109947. https://doi.org/10.1016/j.msec.2019.109947

Gonsalves, A. A.; Araújo, C. R. M.; Soares, N. A.; Goulart M. O. F.; Abreu, F. C. Diferentes estratégias para a reticulação de quitosana. *Quim. Nova.* **2011**, *34* (7), 1215–1223. https://doi.org/10.1590/S0100-40422011000700021

Kumar, M. N. V. R. A review of chitin and chitosan applications. *React. Funct. Polym*. **2000**, *46* (1), 1–27. https://doi.org/10.1016/S1381-5148(00)00038-9

Laranjeira, M. C. M.; Fávere, V. T. Quitosana: biopolímero funcional com potencial industrial biomédico. *Quim. Nova.* **2009**, *32* (3), 672–678. https://doi.org/10.1590/S0100-40422009000300011

Li, H.; Peng, L. Antimicrobial and antioxidant surface modification of cellulose fibers using layer-by-layer deposition of chitosan and lignosulfonates. *Carbohydr. Polym*. **2015**, *124*, 35–42. https://doi.org/10.1016/j.carbpol.2015.01.071

Lins, L. C.; Bazzo, G. C.; Barreto, P. L. M.; Pires, A. T. N. Composite PHB/Chitosan microparticles obtained by spray drying: Effect of chitosan concentration and crosslinking agents on drug release. *J. Braz. Chem. Soc.* **2014**, *25* (8), 1462–1471. https://doi.org/10.5935/0103-5053.20140129

Lu, X.; Chen, Z.; Yu, Q.; Zhu, W.; Li, S.; Han, L.; Yuan, J.; Li, S.; Wu, Y.; Lv, Z.; Chen, B.; You, H. Electrochemical Properties of Chitosan-Modified PbO2 as Positive Electrode for Lead–Acid Batteries. *Energy Technol.* **2022**, *10* (12), 2200910. https://doi.org/10.1002/ente.202200910

Luo, H.; Shen, Q.; Ye, F.; Cheng, Y. F.; Mezgebe, M.; Qin, R. J. Structure and properties of layer-by-layer self-assembled chitosan/lignosulfonate multilayer film. *Mater. Sci. Eng. C.* **2012**, *32* (7), 2001–2006. https://doi.org/10.1016/j.msec.2012.05.023

Marques Neto, J. O.; Bellato, C. R.; Milagres, J. L.; Pessoa, K. D.; Alvarenga, E. S. Preparation and evaluation of chitosan beads immobilized with iron(III) for the removal of As(III) and As(V) from water. *J. Braz. Chem. Soc.* **2013**, *24* (1), 121–132. https://doi.org/10.1590/S0103-50532013000100017

Martínez-Camacho, A. P.; Cortez-Rocha, M. O.; Ezquerra-Brauer, J. M.; Graciano-Verdugo, A. Z.; Rodriguez-Félix, F.; Castillo-Ortega, M. M.; Yépiz-Gómez, M. S.; Plascencia-Jatomea, M. Chitosan composite films: Thermal, structural, mechanical and antifungal properties. *Carbohydr. Polym.* **2010**, *82* (2), 305–315. https://doi.org/10.1016/j.carbpol.2010.04.069

Martins, J. T.; Cerqueira, M. A.; Vicente, A. A. Influence of α-tocopherol on physicochemical properties of chitosan-based filmes. *Food Hydrocoll.* **2012**, *27* (1), 220–227. https://doi.org/https://doi.org/10.1016/j.foodhyd.2011.06.011

Nesic, A. R.; Onjia, A.; Ostojic, S. B.; Micic, D. M.; Velickovic, S. J.; Antonovic, D. G. Novel biosensor films based on chitosan. *Mater. Lett.* **2016**, *167*, 47–49. https://doi.org/10.1016/j.matlet.2015.12.124

Oliveira Junior, O. N.; Raposo, M.; Dhanabalan, A. *Handbook of Surface and Interfaces of Materials*; Academic Press, 2001.

Osiri, H.; Cano, A.; Reguera, L.; Lemus-Santana, A. A.; Regueira, E. Mercury (I) nitroprusside: A 2D structure supported on homometallic interactions, *J. Solid State Chem.* **2015**, *221*, 79–84. https://doi.org/10.1016/j.jssc.2014.09.021

Ottøy, M. H.; Vårum, K. M.; Christensen, B. E.; Anthonsen, M. W.; Smidsrød, O. Preparative and analytical size-exclusion chromatography of chitosans. *Carbohydr. Polym*. **1996**, *31* (4), 253–261. https://doi.org/10.1016/S0144-8617(96)00096-3

Palliani, G.; Poletti, A.; Santucci, A. Vibrational spectrum of sodium nitroprusside. Normal coordinateanalysis for the $Fe(CN)_5NO^{2-}$ ion. *J. Mol. Struct.* **1971**, *8* (1–2), 63–74. https://doi.org/10.1016/0022-2860(71)80043-1

Pannell, M. J.; Doll, E. E.; Labban, N.; Wayu, M. B.; Pollock, J. A.; Leopold, M. C. Versatile sarcosine and creatinine biosensing schemes utilizing layer-by-layer construction of carbon nanotube-chitosan composite films. *J. Electroanal. Chem.* **2018**, *814*, 20–30. https://doi.org/10.1016/j.jelechem.2018.02.023

Picart, C.; Mutterer, J.; Richert, L.; Luo, Y.; Prestwich, G. D.; Schaaf, P.; Voegel, J. C.; Lavelle, P. Molecular basis for the explanation of the exponential growth of polyelectrolyte multilayers. *Proc Natl Acad Sci U S A*. **2002**, *20*, 1–99. https://doi.org/10.1073/pnas.202486099.

Raymond, L.; Morin, F. G.; Marchessault, R. H. Degree of deacetylation of chitosan using conductometric titration and solid-state NMR. *Carbohydr. Res.* **1993**, *246* (1), 331–336. https://doi.org/10.1016/0008-6215(93)84044-7

Roberts, G. A. F. *Chitin Chemistry*; Macmillan Publishers Limite, 1992. https://doi.org/https://doi.org/10.1007/978-1-349-11545-7

Rodrigues, G. D.; Silva, L. H. M.; Silva, M. C. H. Alternativas verdes para o preparo de amostra e determinação de poluentes fenólicos em água. Green alternatives for sample preparation and determination of phenolic pollutants in water. *Quim Nova.* **2010**, *33* (6), 1370–1378. https://doi.org/10.1590/S0100-40422010000600027

Santos, D. S.; Bassi, A.; Rodrigues, J. J.; Misoguti, L.; Oliveira, O. N.; Mendonça, C. R. Light-induced storage in layer-by-layer films of chitosan and an azo dye. *Biomacromolecules*. **2003**, *4* (6), 1502–1505. https://doi.org/10.1021/bm025754f

Sass, N.; Itamoto, C. H.; Silva, M. P.; Torloni, M. R.; Atallah, Á. N. Does sodium nitroprusside kill babies? A systematic review. *Sao Paulo Med. J.* **2007**, *125* (2), 108–111. https://doi.org/10.1590/S1516-31802007000200008

Si, Y.; Park, J. W.; Jung, S.; Hwang, G. S.; Park, Y. E.; Lee, J. E.; Lee, H. J. Voltammetric layer-by-layer biosensor featuring purine nucleoside phosphorylase and chitosan for inosine in human serum solutions. *Sens. Actuators B Chem.* **2019**, *298*, 126840. https://doi.org/10.1016/j.snb.2019.126840

Signini, R.; Campana Filho, S. P. Características e propriedades de quitosanas purificadas nas formas neutra, acetato e cloridrato. *Polímeros*. **2001**, *11* (2), 58–64. https://doi.org/10.1590/s0104-14282001000200007

Signini, R.; Campana Filho, S. P. Purificação e caracterização de quitosana comercial. *Polímeros*. **1998**, *8* (4), 63–68. https://doi.org/10.1590/s0104-14281998000400009

Silva, H. S. R. C.; Kátia, S. C. R.; Ferreira, E. I. Chitosan: hydrossoluble derivatives, pharmaceutical applications and recent advances. *Quim Nova.* **2006**, *29* (4), 776–785. https://doi.org/10.1590/S0100-40422006000400026

Sonne, K.; Dasgupta, P. K. Simultaneous Photometric Flow Injection Determination of Sulfide, Polysulfide, Sulfite, Thiosulfate, and Sulfate. *Anal. Chem.* **1991**, *63* (5), 427–432. https://doi.org/10.1021/ac00005a008

Souza, N. L. G. D.; Salles, T. F.; Brandão, H. M.; Edwards, H. G. M.; Oliveira, L. F. C. Synthesis, vibrational spectroscopic and thermal properties of oxocarbon cross-linked Chitosan. *J. Braz. Chem. Soc.* **2015**, *26* (6), 1247–1256. https://doi.org/10.5935/0103-5053.20150090

Stocche, R. M.; Garcia, L. V.; Reis, M. P.; Miranda, O. Clonidina por via venosa na técnica de hipotensão arterial induzida para timpanoplastias. *Rev. Bras. Anestesiol*. **2003**, *53* (4), 457–466. https://doi.org/10.1590/s0034-70942003000400005

Suginta, W.; Khunkaewla, P.; Schulte, A. Electrochemical biosensor applications of polysaccharides chitin and chitosan. *Chem. Rev.* **2013**, *113* (7), 5458–5479. https://doi.org/10.1021/cr300325r

Swinehart, J. H. The nitroprusside 1. *Coord. Chem. Rev.* **1967**, *2* (4), 385–401. https://doi.org/10.1016/S0010-8545(00)80220-9

Umoren, S. A.; Eduok, U. M. Application of carbohydrate polymers as corrosion inhibitors for metal substrates in different media: A review. *Carbohydr. Polym.* **2016**, *140*, 314–341. https://doi.org/10.1016/j.carbpol.2015.12.038

Ungureanu, C.; Ioniţă, D.; Berteanu, E.; Tcacenco, L.; Zuav, A.; Demetrescu, I. Improving natural biopolymeric membranes based on chitosan and collagen for biomedical applications introducing silver. *J. Braz. Chem. Soc.* **2015**, *26* (3), 458–465. https://doi.org/10.5935/0103-5053.20150298

Vinhola, L.; Facci, T.; Dias, L. G.; Azevedo, D. C.; Borissevitch, G.; Huguenin, F. Self-assembled films from chitosan and poly(vinyl sulfonic acid) on Nafion® for direct methanol fuel cell. *J. Braz. Chem. Soc.* **2012**, *23* (3), 531–537. https://doi.org/10.1590/S0103-50532012000300021

Xia, L.; Long, Y.; Li, D.; Huang, L.; Wang, Y.; Dai, F.; Tao, F.; Cheng, Y.; Deng, H. LBL deposition of chitosan and silk fibroin on nanofibers for improving physical and biological performance of patches. *Int. J. Biol. Macromol.* **2019**, *130*, 348–356. https://doi.org/10.1016/j.ijbiomac.2019.02.147